LBL-29441

Lawrence Berkeley Laboratory
UNIVERSITY OF CALIFORNIA

Physics Division

To be presented at the 3rd International Conference
on Applications of Physics in Medicine and Biology,
Trieste, Italy, September 4–7, 1990, and
to be published in the Proceedings

Digital Radiography: Present Detectors and Future Developments

V. Perez-Mendez

August 1990

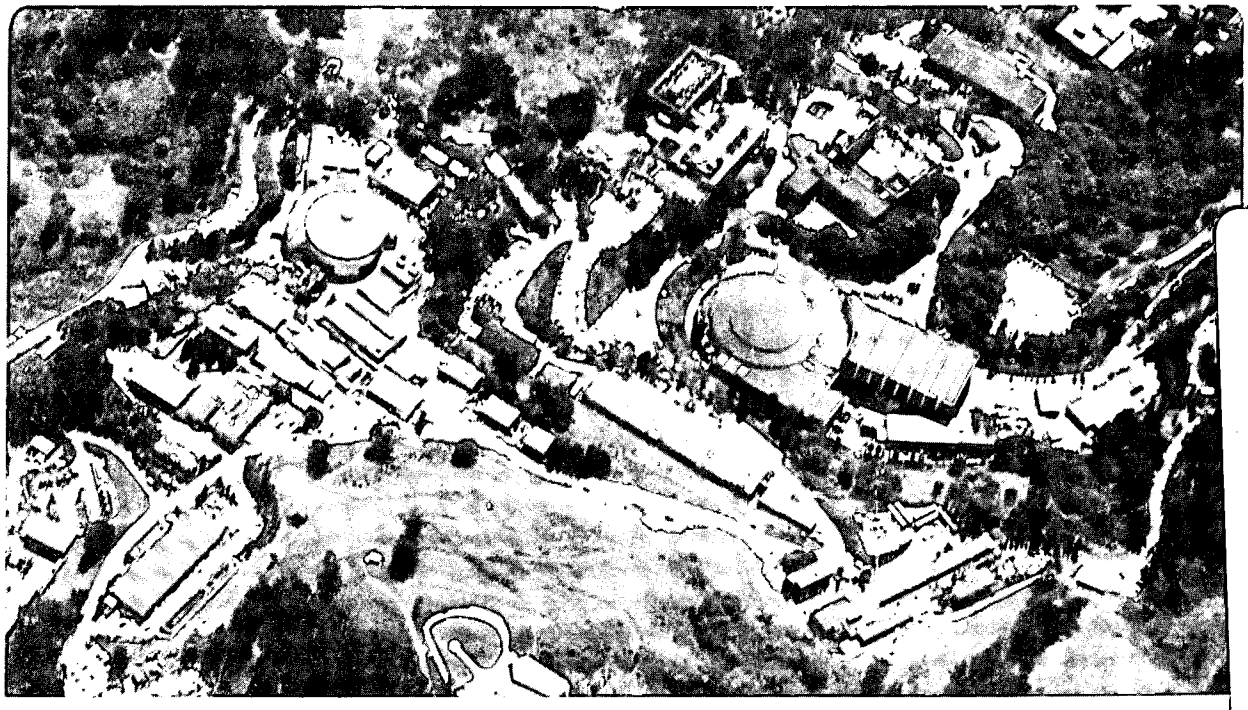

Prepared for the U.S. Department of Energy under Contract Number DE-AC03-76SF00098.

DISCLAIMER

LBL-29441

Digital Radiography: Present Detectors and Future Developments

V. Perez-Mendez
Lawrence Berkeley Laboratory
University of California
Berkeley, CA 94720

August 1990

This work was supported by the Director, Office of Energy Research, Office of High Energy and Nuclear Physics, High Energy Physics Division, of the U.S. Department of Energy under Contract No. DE-AC03-76SF00098.

LBL 29441

August 1990

DIGITAL RADIOGRAPHY: PRESENT DETECTORS AND FUTURE DEVELOPMENTS

V. Perez-Mendez
Lawrence Berkeley Laboratory, University of California
Berkeley, CA 94720 USA

ABSTRACT

Present detectors for digital radiography are of two classes: real time detectors and storage (non real time) types. Present real time detectors consist of image intensifier tubes with an internal cesium iodide layer x-ray converter. Non real time detectors involve linear sweep arrays or storage detectors such as film. Future detectors discussed here can be of both types utilizing new technologies such as hydrogenated amorphous silicon photodiode arrays coupled to thin film transistor arrays.

INTRODUCTION

Digital radiography for special applications in medical imaging has been utilized for over 20 years in various forms. The rapid development of small computer technology, new radiation detectors, and of high resolution electronic display devices has increased the use of digital radiography to many general purpose medical imaging situations. This technology may in fact supplant the conventional x-ray film usage completely and thus simplify the film storage and retrieval problems facing large medical organizations(1). Present day digital radiography x-ray machines generally use image intensifier tubes with an internal layer of $CsI(Na)$ as the detector. These types of image intensifier tubes have also been used in bi-plane angiography machines in which the images were recorded on 35 or 70 mm movie film. Some modern x-ray machines equipped with two x-ray sources and two image intensifier detectors - shown in Fig. 1 - can fulfill the dual functions of

angiography and digital radiography since their output is digital and can thus be stored in magnetic tape or digital optical disks, for both functions. In the following sections we cover the properties of image intensifier detector systems which are the presently available real time detectors. Next we discuss line sweep detector devices which are partially real time; then non real time devices using Fuji scintillator detector screens and film detection. Finally, we discuss future flat screen pixel detector devices utilizing scintillator layers coupled to amorphous silicon photodiode layers deposited on a substrate which has the amplifying and routing thin film (TFT) a-Si:H or polysilicon electronics on it.

II IMAGE INTENSIFIER DETECTORS

A typical image intensifier tube is shown in Fig. 1b. Sizes used in radiology range from 20-30cms diameter sensitive imaging area. Figs. 2a shows schematically the internal structure of these tubes. The x-ray sensing component is a vacuum evaporated layer of cesium iodide activated with sodium ($C_SI(Na)$) (Fig. 2b). This is deposited on a spherical aluminum shield. A thin metal or transparent layer of M_gO, or tin oxide is deposited on the front surface and forms the base for the photocathode. The photocathodes used include cesium antimonide (C_SS_b) or other cesium based photocathodes. The photocathode is held at some suitable potential relative to the focussing and accelerating electrodes of the tube. The output is a scintillator layer deposited on the exit glass window. For non digital angiography this window is viewed by a movie camera. For digital recording a charge coupled device (CCD) is used. A critical element is the $C_SI(Na)$ layer(2,3,4,5). This is deposited on the aluminum spherical surface which is held at 100 ~150°C during the manufacturing process. When the aluminum substrate cools down, the $C_SI(Na)$ forms columnar structures which tend to collimate the scintillation light. A better columnar structure is obtained if the aluminum substrate surface is textured by mechanical or chemical means. The columnar structure is shown in Fig. 3. Typical widths of these

columns range from 20-50 μm. The light collimating characteristics are shown in Fig. 4. The overall spatial resolution of the device is shown in the modulation transfer curves of Fig. 2c and is quoted by the manufacturers as 4-6 line pairs/mm. The CsI (Na) scintillator emits ~38000 visible light photons/MeV of absorbed energy (6). Although CsI(Tl) emits more light (50000 visible photons/MeV), the CsI(Na) is used since its spectral response is a better match to the Cs -Sb photocathode. The light emission spectra of CsI(Na) and CsI(Tl) are shown in Fig. 5a with the response curve of a Cs-Sb photocathode and the response of an amorphous silicon photodiode. Figure 5b shows the x-ray conversion efficiency of these layers. When we have amorphous silicon photodiode array detectors, discussed in Section IV, it is better to use CsI(Tl) because of its higher light output, less hygroscopic properties than CsI(Na) and because its response curve - as shown in Fig. 5a is a better match to the CsI(Tl). The lifetime of these image intensifier tubes is in excess of 5 years with normal clinical use. The CsI scintillator can be damaged by exposure to the x-ray radiation. In Fig. 6 we show some radiation damage results on exposure to C_o-60 γ rays on CsI(Tl), indicating that the intensifier tubes can be used for over 10^5 RAD exposures. Presently available digital/angiography x-ray machines using the image intensifier tubes are very reliable. The minor disadvantages of the image intensifier detectors are their bulk, cost, and limited spatial resolution.

III ALTERNATIVE DIGITAL RADIOGRAPHY DETECTION SCHEMES

The three detector methods discussed in this section are (a) small optical laser sweep scans of image intensifiers, (b) full size scintillator-optical photodiode scan devices, and (c) static detector devices - Fuji laser scanned scintillator plates.

(a) In these devices (7), the output of a conventional x-ray image intensifier is viewed at the output screen by a linear diode array. The imager is shown schematically in Fig. 7a and

have been applied to mammography and detailed scanning of small regions (8). The x-ray beam is collimated by a slit which is synchronized with the motion of the linear photo diode array at the output of the image intensifier. The use of a slit source of x-rays couped to linear detector minimizes radiation exposure and improves the image contrast by eliminating the out of plane scatter of the x-rays in traversing the object. The photodiode arrays which have been used in these applications have up to 1024 sensor elements on 25 μm centers and have been shown to have a spatial resolution > 8 line pairs/mm (9).

(b) Full size scintillator-optical photodiode scan devices.

These have been proposed during the last few years (10) and prototype devices have been made. Fig. 7b shows a schematic line detector digitizer. The line detector usually has a scintillator mounted on a crystalline silicon photodiode array. This configuration has also been used for x-ray inspection of moving objects such as luggage at airport security checkpoints (11). This scheme has the disadvantage in that it takes > 0.1 sec to read out a full frame. This is relatively unimportant for brain scans and for other static medical imaging applications except for angiography when small blood vessels on the moving heart are imaged. This difficulty could be minimized by synchronizing the detector sweep with an EKG trigger signal and summing up over a number of heart beats. If the x-ray tube is also equipped with a small lead slit which is mechanically coupled to the detector strip and moves in unison with it (Fig. 7c), patient dose and image degradation from out-of line scatters is considerably reduced.

(c) Rapid Scan Static Devices - Fuji Imaging Screen

Fuji research developed some years ago (12) an x-ray imaging screen with a photostimulable phosphor which stores x-ray intensity information for many hours. The stored light intensity is then read out by a scanning laser beam and the data can be stored

digitally. The photostimulable phosphor is a $B_aFX(Eu)$ (x can be Cl, Br, I) compound which releases the stored energy as visible light in the 350 -450 nm wavelength range. The scanning is done with a 633 nm helium-neon laser. The screen-readout is shown schematically in Fig. 8a. Fib. 8b shows the structure of the film. Fig. 8c shows the laser scanning device which produces a signal which is subsequently digitized. Figure 9a shows the wavelength for stimulation-readout of the phosphor and the emission output band. Fig. 9b gives the x-ray sensitivity for a 10 μm B_aFX layer and Fig. 9c shows the spatial accuracy of the system.

The dynamic range over which the light output is linearly proportional to the x-ray absorbed intensity ranges from 10^{-3} - 10^3 mR. With a good linear signal versus x-ray response, digital subtraction radiography can be done accurately. Compared to conventional film which has been used in the past for contrast agent subtraction images, the Fuji screens have the advantage the (a) they do not require any processing and developing (b) they have a large dynamic range (c) their output is quite linear and (d) the laser readout is considerably faster than film densitometer readout.

IV FLAT SCREEN DEVICES BASED ON AMORPHOUS SILICON TECHNOLOGY :

Hydrogenated amorphous silicon (a-Si:H) is a material whose capability for producing p, n junctions and thereby making electronic devices was recognized in 1976 (13). Since then it has been developed as the most widely used material for solar cells. Further more, a technology for making thin film transistors from a-Si:H has lead to their use also in flat television screens, in facsimile machine readout heads, and in electrocopying machines (10). Hydrogenated amorphous silicon layers can be readily made in large areas > 50 x 50 cms by decomposition of silane in a plasma enhanced chemical vapor deposition machine (PECVD). The addition of small (10^{-2}) concentrations

of diborane (B_2H_6) or phosphine (PH_3) to the silane gas produces p or n doped layers respectively. The intrinsic (*i*) material has the best transport electrical characteristics and hence the bulk of the a-Si:H diodes consist of thin (~20 nm) p, n layers next to the metal contacts with a thicker (>1μm) intrinsic layer sandwiched in between. Hydrogenated amorphous silicon p-i-n diodes when reverse biased form excellent photodiodes due to the fact that the mean free path for light absorption is small , < 1.5 μm, over the visible range and therefore a high detection efficiency is achieved. The detection efficiency is shown in Fig. 5a. The electrons and holes which are produced by the light absorption are collected with efficiencies >90% from the i layer. The metal contact and the thin p layer produce some losses which are minimized by using indium tin oxide (ITO) transparent conducting layers in place of metal and keeping the p layer small compared to the mean free path for light absorption. Typical pixel diode arrays with their associated thin film transistors, as used in facsimile machine readers have pixel dimensions of ~70 x 70 μm: the dimensions of the individual pixels are determined by lithographic etching of the top ITO contact. In order to convert such a linear device to a linear x-ray sweep detector it has to be coupled to a suitable x-ray sensitive scintillator. Many possible scintillators are available such as the intensifying screens used in x-ray film cassettes. These Lanex (Kodak) and Chronex (Dupont) screens have rare earth scintillators. For better light collimation fibre optic plates with rare earth scintillators such as terbium or cerium are commercially available with fiber sizes as small as 20 μm (11). A third possibility which we are developing in a joint LBL-Xerox Palo Alto collaboration is to use $CsI(Tl)$ 300-400 μm thick layers with columnar structures similar to the $CsI(Na)$ used in the image intensifiers. A two dimensional 128 x 128 photodiode array that is under development at Xerox Palo Alto Research Lab for charged particle and x-ray detection is shown in Fig. 10. The array is read-out line by line onto a low noise, fast linear integrated circuit chip with 128 inputs. This device is the SVX chip developed at the Lawrence Berkeley Laboratory for high energy physics applications. The 128 inputs are low noise, charge sensitive inputs which can read out each pixel in ~ 1

μsec. Thus to read out a complete 128 x 128 array will require ~ 16.5 milliseconds. Our present arrays have pixel sizes of 300 x 300 μm and 1 x 1 mm. This technology is also capable of producing 50 x 50 μm pixel sizes. Thus in order to cover the area needed for digital radiography (30 x 30 cm - as in present image intensifiers) we would have to stack a number of these to cover the full area.

V SUMMARY AND CONCLUSIONS

For real time digital radiography, image intensifiers with a spatial resolution of 4-5 line pairs/mm are the standard tool of the industry. Linear sweep arrays using crystal silicon or amorphous silicon detectors are used in prototype devices as possible substitutes for the image intensifiers. The Fuji laser scanned scintillation screen is a high quality good resolution non real time detector with a spatial resolution 4-10 line pairs/mm. Flat area pixel devices utilizing amorphous silicon diode arrays coupled to thin film a-Si:H transistors are under development as future substitutes for x-ray film.

Acknowledgements: I would like to thank my colleagues at LBL who have participated in the amorphous silicon work: G. Cho, J. Drewery, I. Fujieda, S. N. Kaplan, S. Qureshi, D. Wildermuth, as well as R. A. Street and S. Nelson from Xerox Palo Alto

This work was supported by the Director, Office of energy Research, Office of High energy and Nuclear Physics, Division of High Energy Physics, of the US Department of Energy under Contract No. DE-AC03-76SF00098.

REFERENCES

(1) W. J. Dallas, IEEE Spectrum (april 1990) 33-36

(2) C. W. bates, Adv. Electronics & Electron Phys., 28A (1969) 451-459

(3) A.L.N. Stevels and A. D. M. Schrama-de-Pauw, Phillips Res. Reports 29 (1974) 340-352, 29 (1974) 353-362

(4) U.S. Patents Awarded to Phillips 1423935 (1974), 4731558 (1988), 4725724 (1988)

(5) H. Washida and T. Sonoda, Adv. Electronics & Electron Phys. 52 (1979) 201-207.

(6) I. Holl, E. Lorenz and G. Mageras. IEEE Trans. Nuc. Sci., NS 35 (1988) 105-109

(7) R. M. Nishikawa, G. E. Mawdsley, A. Fenster and M. J. Yaffe, Med Phys 14 (1987) 717-727

(8) I. A. Cunningham, B. B. Hobbs, R. K. Gerson and A. Fenster, SPIE Vol 767. Medical Imaging (1987) 186-194

(9) Application Notes, Solid State Line Scanners, E.G.& G. Reticon, Sunnyvale, California

(10) B. Munier, G. Roziere, P. Prieru-Drevon, H. Rougeot, SPIE vol. 1090. Medical Imaging III: Image Formation (1989) 257-262

(11) E. Ellin (Scantech Corp.), Advanced Imaging (1988) 28-32

(12) M. Sonoda, M. Takano, J. Miyahara, H. Kato, Radiology 148 (1983) 833-838

(13) W. E. Spear and P. G. Lecomber, Phil. Mag 33 (1976) 935-949

(14) Semiconductors and Semimetals, Vol. 21 (parts A,B,C,D), Academic Press 1984

(15) Synergistic Detector Design, Mountain View, CA 94043. Collimated Holes, Campbell, CA 95008

(16) R. A. Street, S. Nelson, L. Antonuk and V. Perez-Mendez, to be published Materials Research Society, Vol. 192 (Oct. 1990)

(17) S. A. Kleinfelder, W. C. Carithers, R. P. Ely, C. Haber, F. Kirsted, H. C. Spieler, IEEE Trans. Nuc. Sci. NS-35 (1988) 171-175

FIGURE CAPTIONS

Figure 1: (a) Photograph of Shimadzu Corp (Kyoto, Japan) biplane x-ray machine for angiography and digital x-ray detection
(b) Photograph of Shimadzu 30 cm image intensifier

Figure 2: (a) Schematic cross section of image intensifier tube
(b) Schematic of CsI(Na) layer and photocathode
(c) Modulation transfer curves for Shimadzu image intensifier

Figure 3: CsI(Na) layers showing columnar structure
(a) Temperature formed columns
(b) Etched substrate formed columns

Figure 4: Light spread from CsI(Na) columnar layers

Figure 5: (a) Light emission spectra of CsI(Na) and CsI(Tl)
(b) X-ray detection efficiency of 100, 300, 500 μm CsI layer

Figure 6: Radiation damage to CsI(Tl) layer. Columnar structure CsI.

Figure 7: (a) Line scan of image intensifier
(b) line scan (Scantech)
(c) Line scan: x-ray detector motion synchronizer

Figure 8: (a) Fuji screen system
(b) Fuji screen film structure
(c) Fuji screen laser digitizing readout

Figure 9: (a) Fuji screen stimulation and emission spectra
(b) Absorption of x-rays
(c) Spatial resolution of system: MTF

Figure 10: Two dimensional photodiode array a-Si:H. the output device is the LBL SVX chip which has 128 parallel, charge sensitive amplifier inputs.

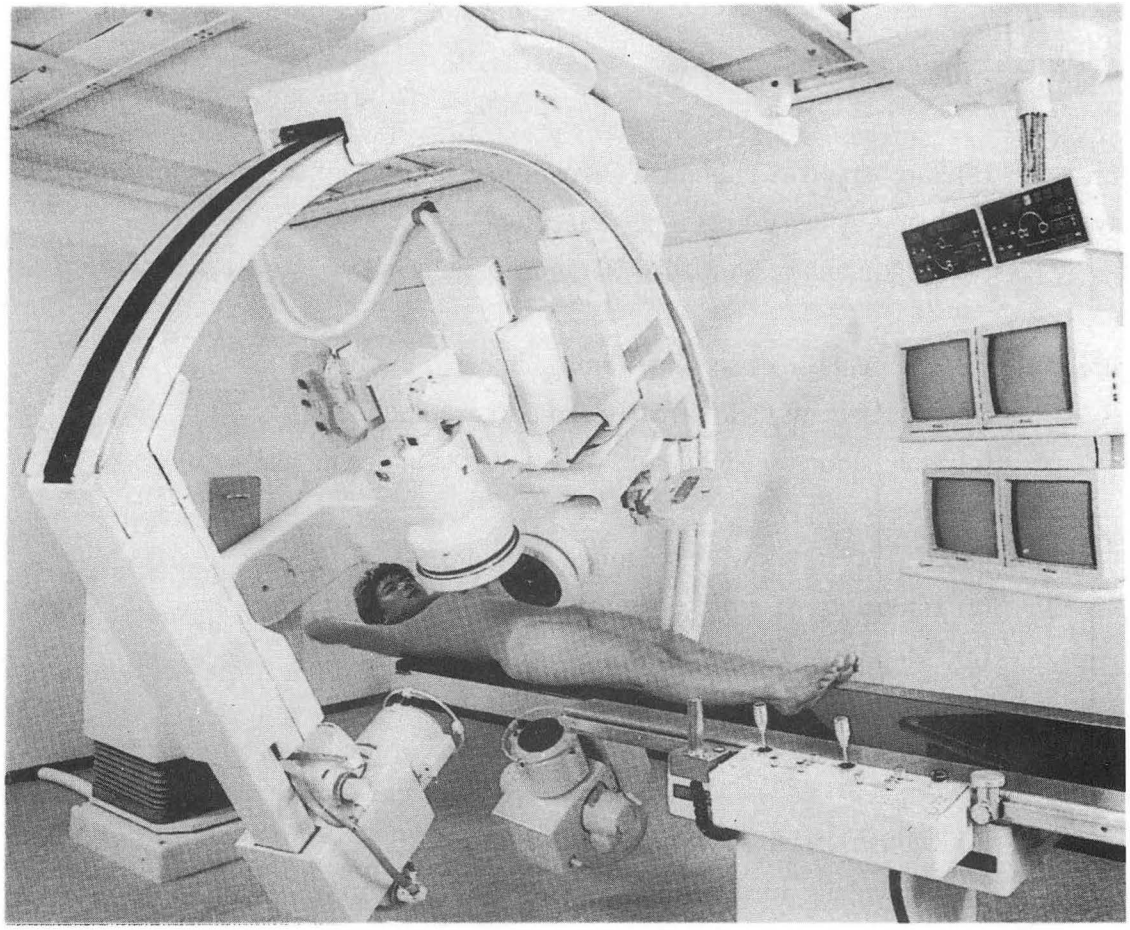

Fig. 1(a)

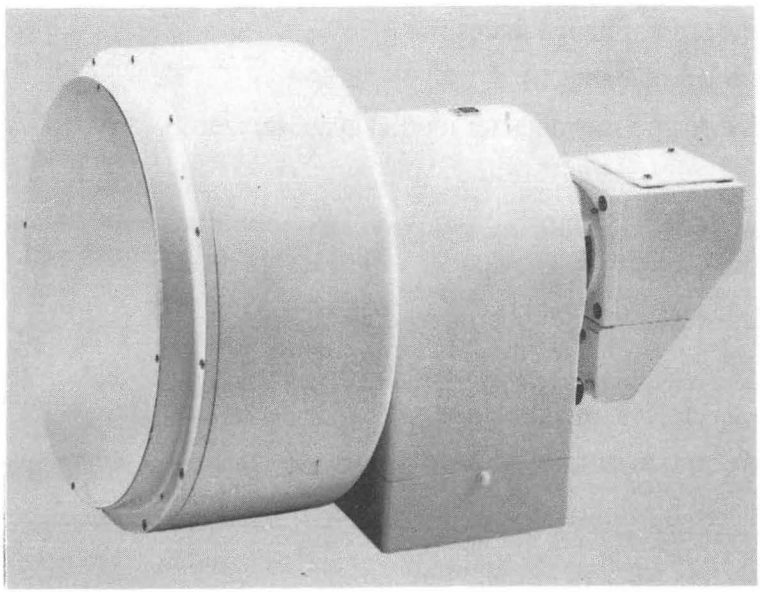

Fig. 1(b)

X-ray Image Intensifiers

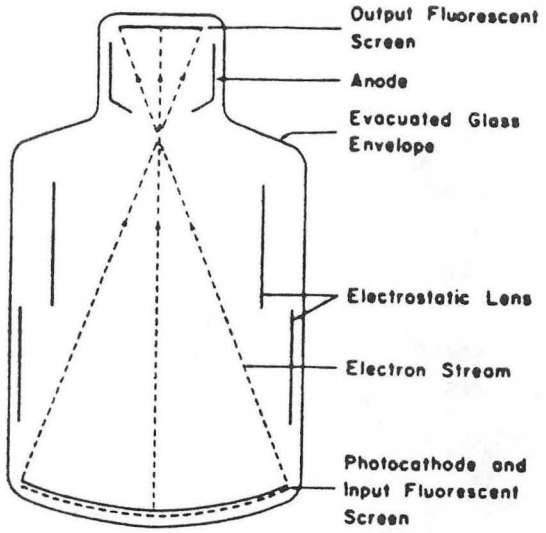

X-ray image intensifier tube

(a)

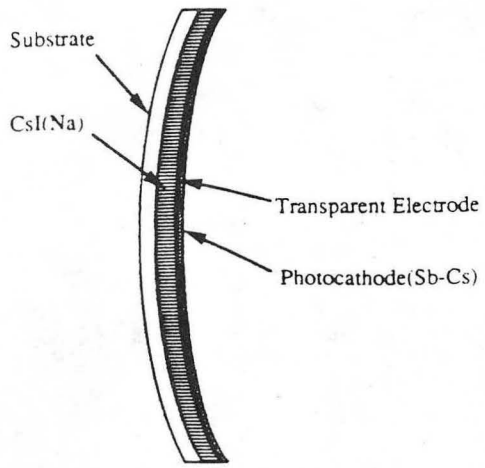

(b)

Items	Unit	Performance
Nominal entrance field size	cm	30–23–15
Conversion factor <(cd/m²)/(μc/kg·s)>		640
Resolution 30cm/15cm	lp/cm	38·52
Contrast ratio		30
Image distortion	%	Less than 7
Output image size	mm	30 ± 0.5
Power requirement (50/60Hz)		Single phase AC100V ± 10% below 100W

MTF (at the center) of IA-12/6MTW [typical values]

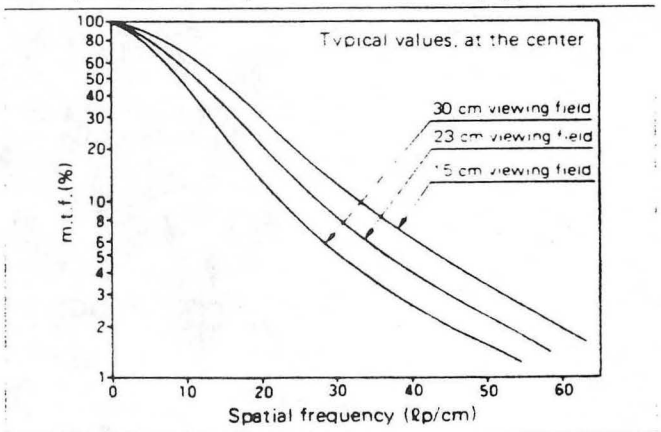

Fig. 2(c)

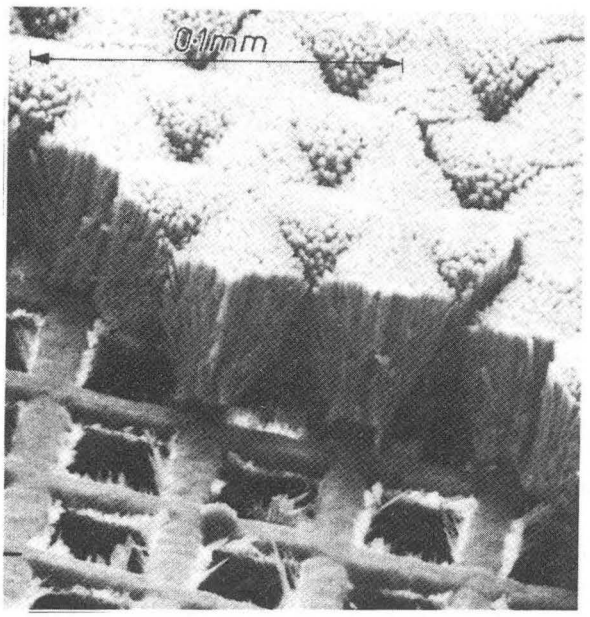

(a)

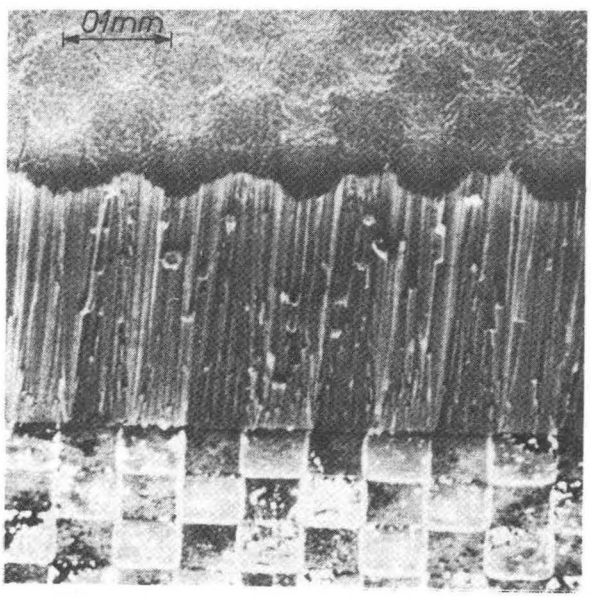

Fig. 3(b)

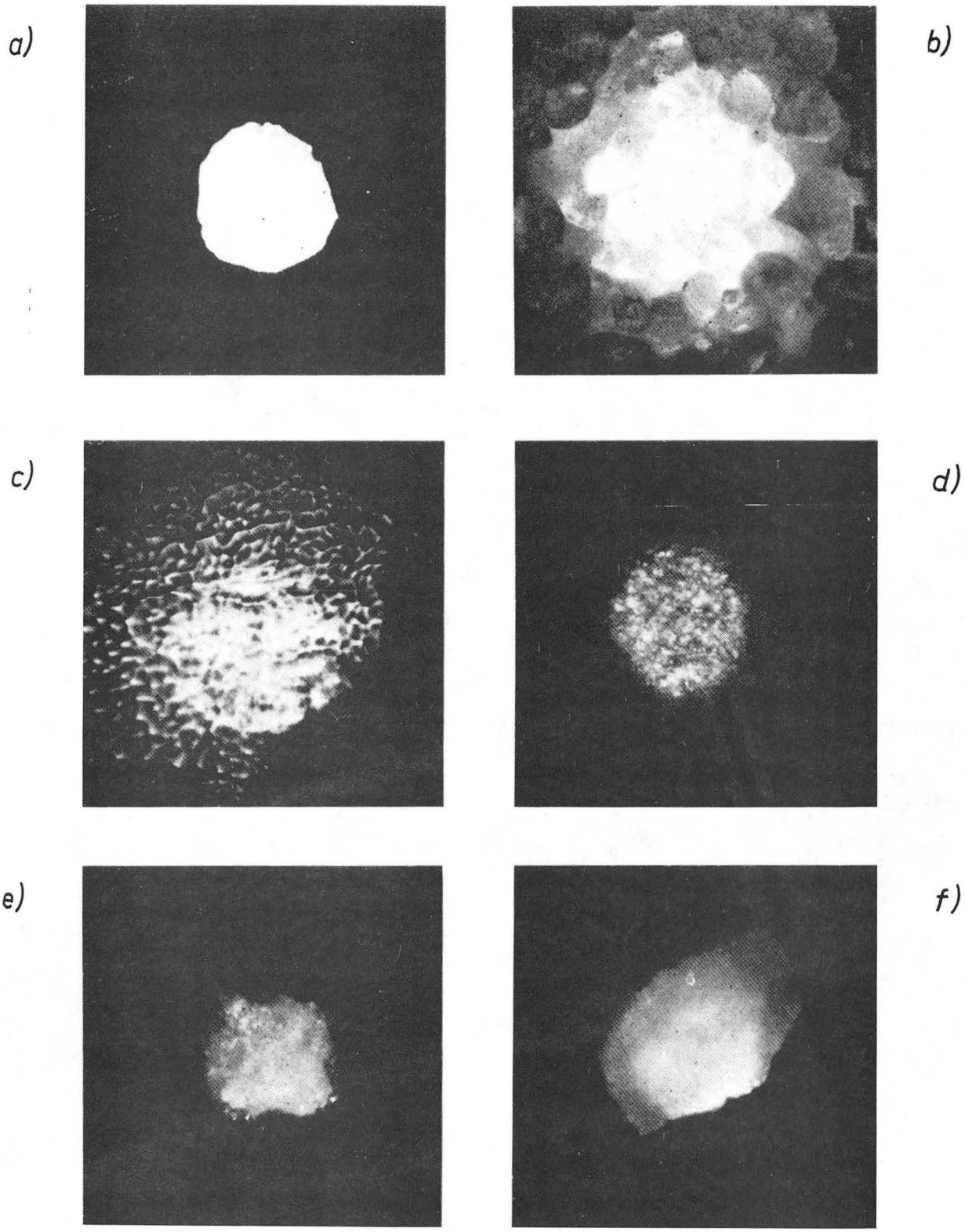

Reprinted with permission of Philips Journal of Research (Philips Research Report 29 (1974) pp. 353-362).

Comparison of lateral light scattering in various types of screens. Picture (*a*) shows the light spot impinging on the screens, (*b*) gives the distribution of the light after reflection from a (Zn,Cd)S:Ag screen, (*c*) by a CsI:Na screen without cracks, (*d*) of a similar screen with cracks; (*e*) shows the distribution after reflection from a CsI:Na screen with the regular crack pattern of a photo-etched substrate, (*f*) that of a layer on a wire-gauze substrate.

Fig. 4

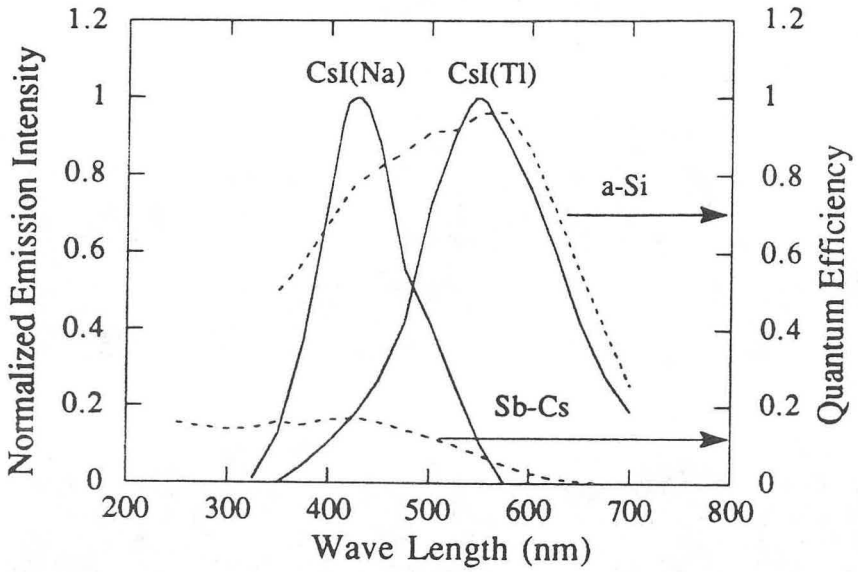
Normalized Emission Intensity
Quantum Efficiency
CsI(Na)
CsI(Tl)
a-Si
Sb-Cs
Wave Length (nm)
1.2
1
0.8
0.6
0.4
0.2
0
200
300
400
500
600
700
800

(a)

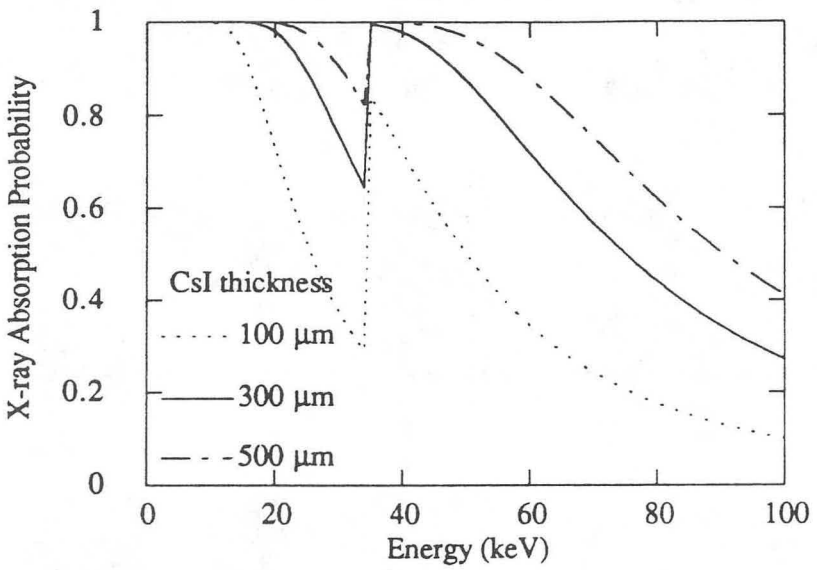
X-ray Absorption Probability
CsI thickness
100 μm
300 μm
500 μm
Energy (keV)
1
0.8
0.6
0.4
0.2
0
0
20
40
60
80
100

(b)

Fig. 5

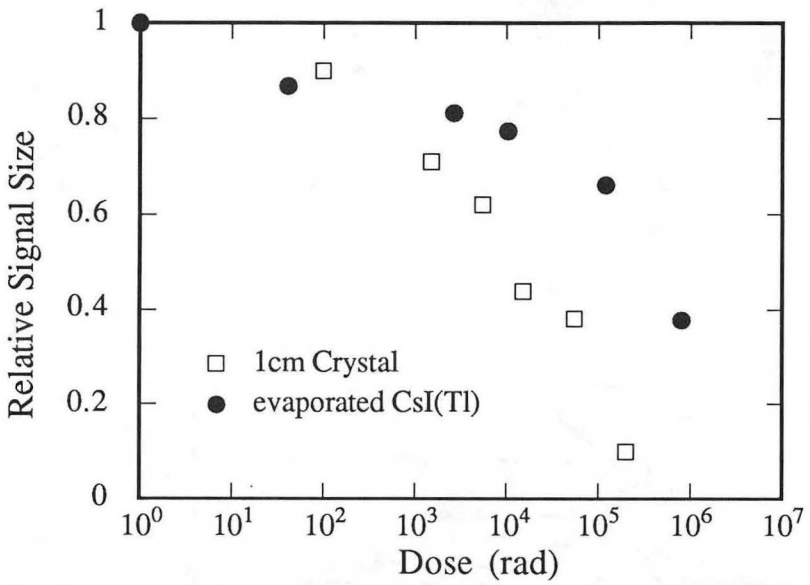
Relative Signal Size
1
0.8
0.6
0.4
0.2
0
1cm Crystal
evaporated CsI(Tl)
10^0 10^1 10^2 10^3 10^4 10^5 10^6 10^7
Dose (rad)

(a)

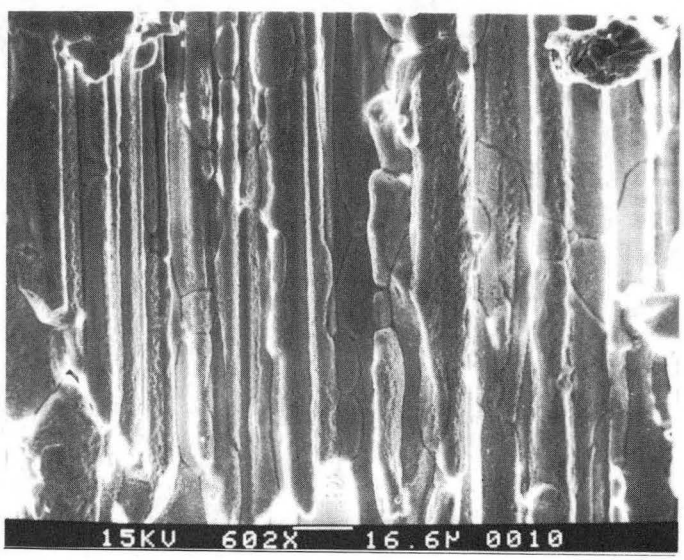
15KV 602X 16.6P 0010

(b)

Fig. 6

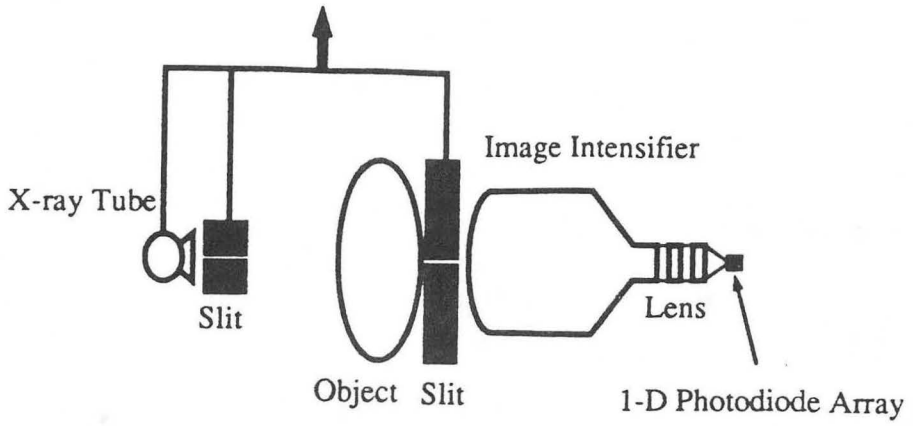
X-ray Tube
Slit
Image Intensifier
Lens
Object
Slit
1-D Photodiode Array

(a)

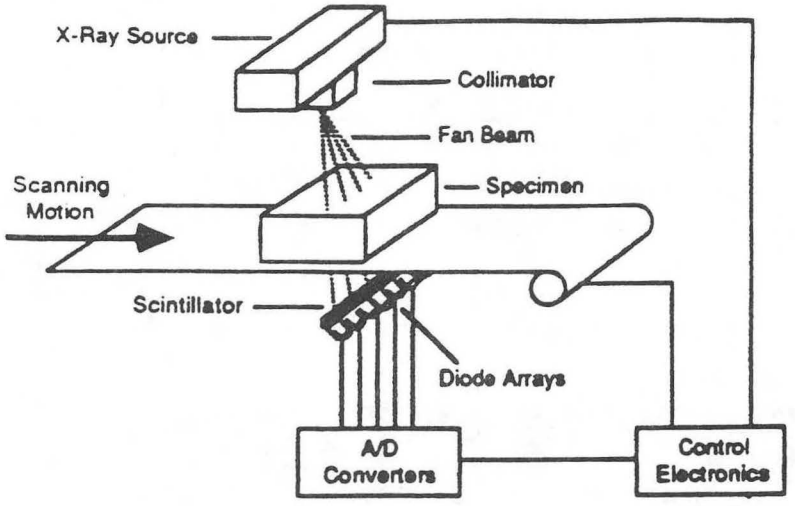
X-Ray Source
Collimator
Fan Beam
Specimen
Scanning Motion
Scintillator
Diode Arrays
A/D Converters
Control Electronics

(b)

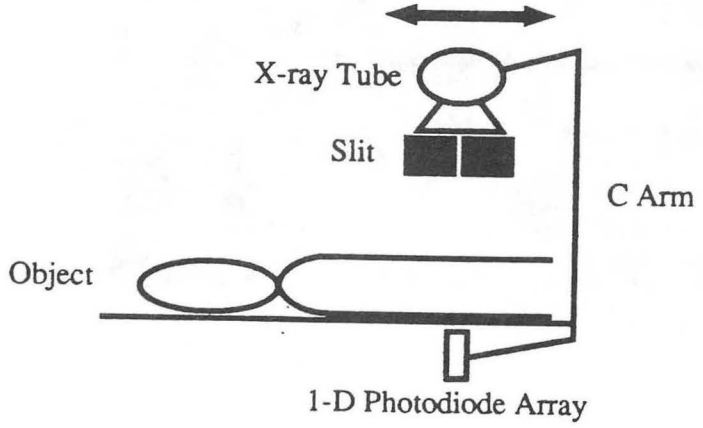
X-ray Tube
Slit
C Arm
Object
1-D Photodiode Array

(c)

Fig. 7

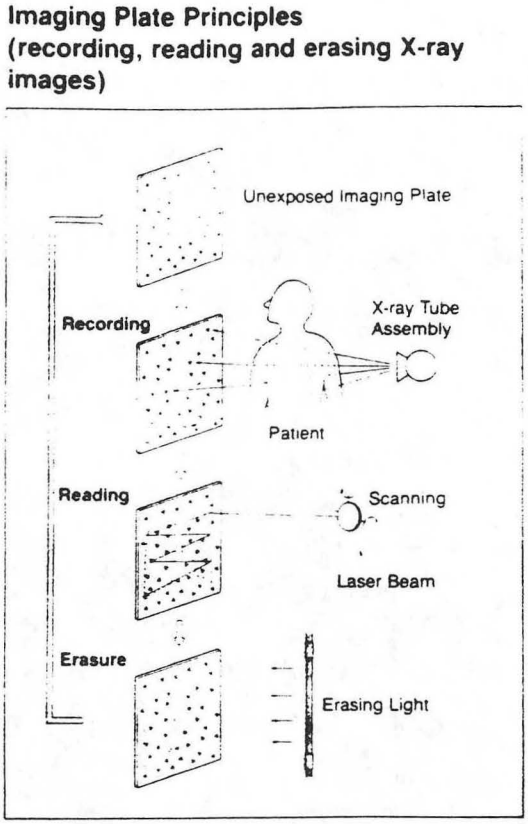
Imaging Plate Principles
(recording, reading and erasing X-ray images)
Unexposed Imaging Plate
Recording
X-ray Tube Assembly
Patient
Reading
Scanning
Laser Beam
Erasure
Erasing Light

(a)

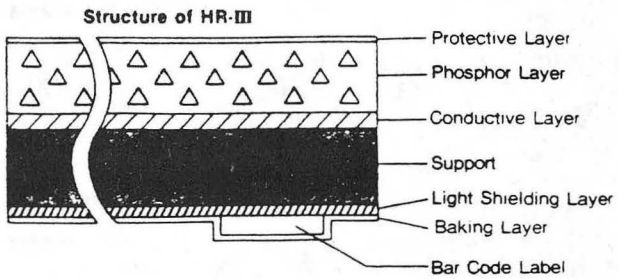
Structure of HR-III
Protective Layer
Phosphor Layer
Conductive Layer
Support
Light Shielding Layer
Baking Layer
Bar Code Label

(b)

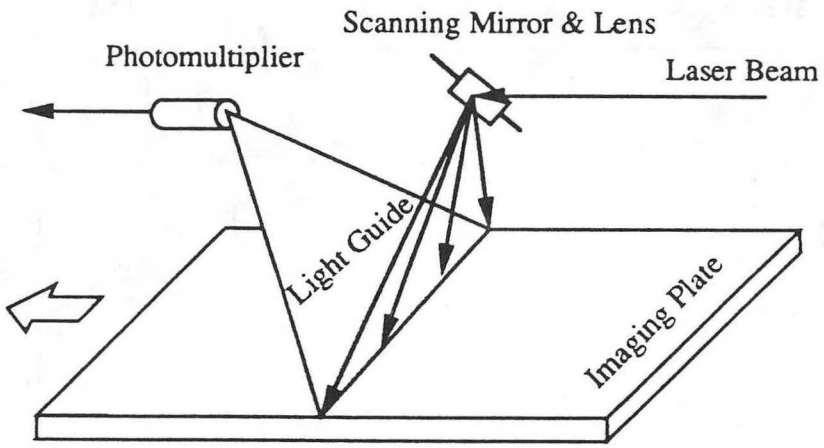
Scanning Mirror & Lens
Photomultiplier
Laser Beam
Light Guide
Imaging Plate

(c)

Fig. 8

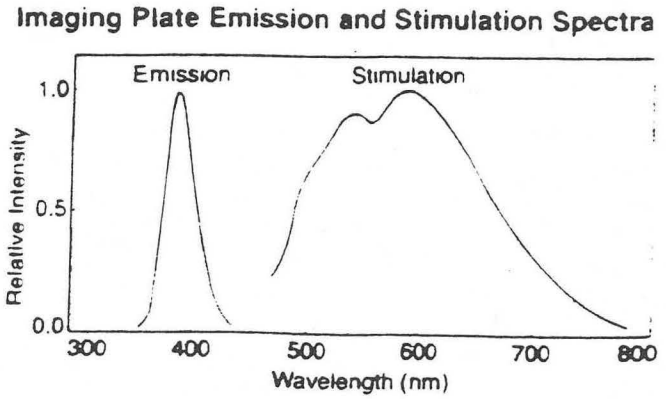
Imaging Plate Emission and Stimulation Spectra
Emission
Stimulation
Relative Intensity
1.0
0.5
0.0
300
400
500
600
700
800
Wavelength (nm)

(a)

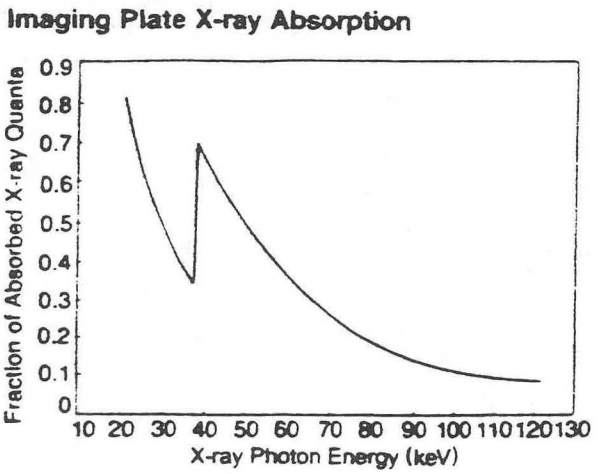
Imaging Plate X-ray Absorption
Fraction of Absorbed X-ray Quanta
0.9
0.8
0.7
0.6
0.5
0.4
0.3
0.2
0.1
0
10 20 30 40 50 60 70 80 90 100 110 120 130
X-ray Photon Energy (keV)

(b)

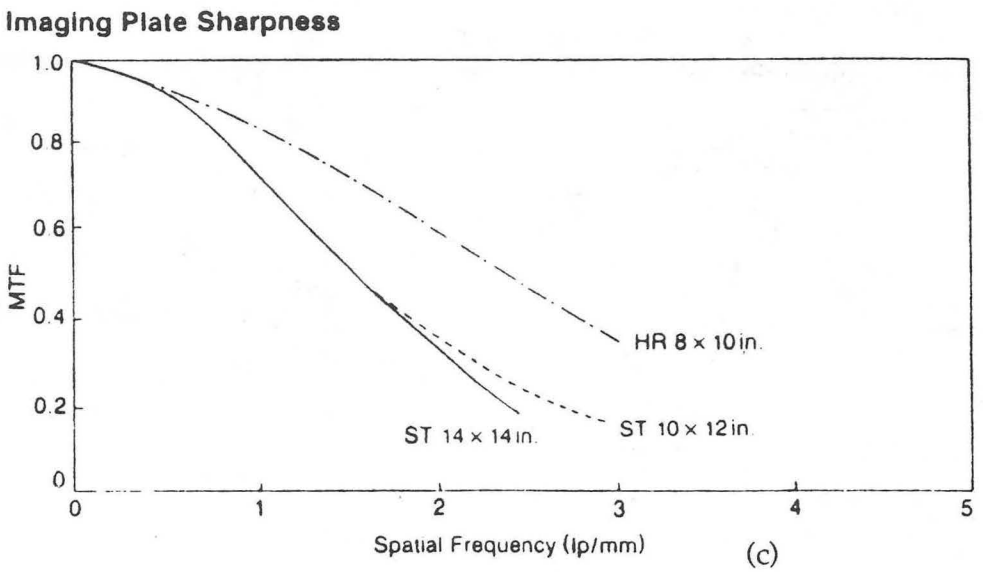
Imaging Plate Sharpness
MTF
1.0
0.8
0.6
0.4
0.2
0
0
1
2
3
4
5
Spatial Frequency (lp/mm)
HR 8 x 10 in.
ST 10 x 12 in.
ST 14 x 14 in.

(c)

Fig. 9

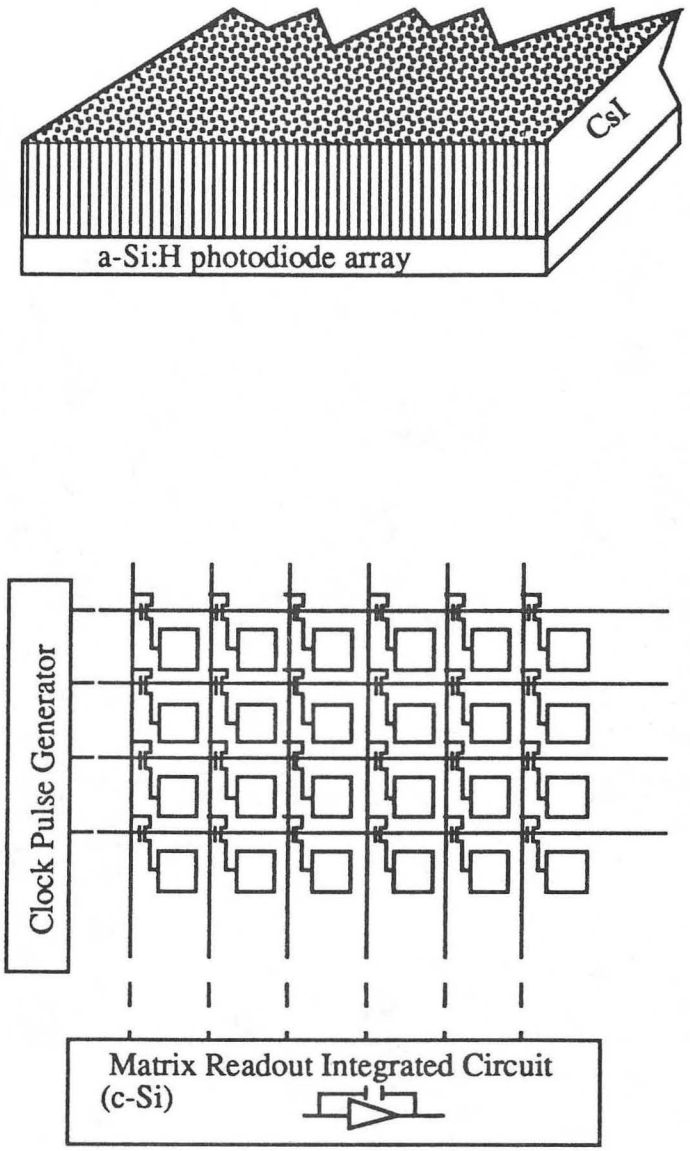
CsI
a-Si:H photodiode array
Clock Pulse Generator
Matrix Readout Integrated Circuit
(c-Si)

Fig. 10

LAWRENCE BERKELEY LABORATORY
UNIVERSITY OF CALIFORNIA
INFORMATION RESOURCES DEPARTMENT
BERKELEY, CALIFORNIA 94720